International Research Journal of Pure and Applied Chemistry

Volume 25, Issue 5, Page 1-16, 2024; Article no.IRJPAC.119483
ISSN: 2231-3443, NLM ID: 101647669

Preparation and Characterization of Two Modified Laterite Soils for Arsenic Removal in Aqueous Solutions: Efficiency and Kinetic Modelling

Rasmané Tiendrébéogo [a,b], Yacouba Sanou [a*], Raymond Kaboré [a], Samuel Paré [a] and Aboubacar Senou [b]

[a] Laboratory of Analytical, Environmental and Bio-Organic Chemistry, University Joseph KI, ZERBO, 03 BP 7021 Ouagadougou 03, Burkina Faso.
[b] Laboratory of Mineral, Water and Environment Analysis, SENEXEL BP312 Ouagadougou Kossyam, Burkina Faso.

Authors' contributions

This work was carried out in collaboration among all authors. All authors read and approved the final manuscript.

Article Information

DOI: https://doi.org/10.9734/irjpac/2024/v25i5871

Open Peer Review History:
This journal follows the Advanced Open Peer Review policy. Identity of the Reviewers, Editor(s) and additional Reviewers, peer review comments, different versions of the manuscript, comments of the editors, etc are available here: https://www.sdiarticle5.com/review-history/119483

Original Research Article

Received: 02/06/2024
Accepted: 05/08/2024
Published: 24/08/2024

ABSTRACT

Consumption of arsenic-contaminated water is the cause of major problems such as melanosis, hyperkeratosis and cancer. To mitigate this pollution, this study was carried out using analytical methods to prepare chemically treated laterite (TL) and chemically doped laterite with ferrihydrite (DL). The adsorbents were characterized using scanning electron microscopy (SEM), X-ray

**Corresponding author: E-mail: prosperyacson@gmail.com;*

Cite as: *Tiendrébéogo, Rasmané, Yacouba Sanou, Raymond Kaboré, Samuel Paré, and Aboubacar Senou. 2024. "Preparation and Characterization of Two Modified Laterite Soils for Arsenic Removal in Aqueous Solutions: Efficiency and Kinetic Modelling". International Research Journal of Pure and Applied Chemistry 25 (5):1-16. https://doi.org/10.9734/irjpac/2024/v25i5871.*

diffraction (XRD), Fourier transform infrared spectroscopy (FTIR), inductively coupled plasma atomic emission spectrometry (ICP-AES), X-ray fluorescence (XRF) and the Brunauer Emmett Teller (BET) method. The specific surface area, bulk density and pH at zero charge point (pH_{PZC}) of TL and DL ranged from 81.306 to 40.099 m^2/g, from 1.67 to 2.27 and from 5.41 to 8.02, respectively. The $SiO_2/(Fe_2O_3 + Al_2O_3)$ ratio was 0.31 for TL and 0.20 for LD, showing that the materials prepared were still classified as laterite adsorbents. Experimental results from batch experiments on the removal of arsenic species (As (III)) and arsenic (As (V)) using two adsorbents showed the strong influence of operating conditions such as pH, initial concentration, adsorbent dose and contact time. The isotherm modelling concluded that the removal of arsenic species was occurred by multilayer adsorption on the heterogenous surfaces of laterites. For the removal of As(V), the maximum adsorption capacity was 7.36 and 9.79 mg/g for TL and DL, respectively, while for the removal of As (III), the adsorption capacity for TL and DL was 5.17 and 7.89 mg/g, respectively. The kinetic study of the adsorption of As(V) or As(III) on modified laterites concluded that the process was described by the pseudo-second-order model, with a chemisorption process to be explored.

Keywords: Adsorbent; arsenic; adsorption; ferrihydrite; laterite; removal.

1. INTRODUCTION

The alteration of rocks, whether due to natural processes or human activities, can result in the release of heavy metals and metalloids like arsenic into the environment [1,2]. Drinking water contaminated with arsenic can have effects on health such as pigmentation, hyperkeratosis, and ulceration), as well as respiratory, pulmonary, cardiovascular, gastrointestinal, hematological, hepatic, renal, reproductive, and immunological changes [3,4]. Arsenic exists in two common forms: As (III) and As (V), with As (III) being less commonly found in water but more toxic than As (V) [4]. Research conducted by Bretzler *and al.* [5] revealed that approximately 560,000 individuals in Burkina Faso may be at risk of exposure to arsenic-contaminated water. Previous works showed some cases of hyperkeratosis and melanosis have been observed in several villages of Burkina Faso, including Tanlili, Essakane, and Mogtédo [6, 7]. To address this public health concern, various techniques have been developed to reduce the level of arsenic in water including filtration, coagulation precipitation, reverse osmosis, electrodialysis, adsorption, and combination methods [4, 8]. Adsorption, in particular, is shown as an effective method for treating water contaminated with arsenic, especially using adsorbent materials [8, 9]. Among the adsorbent's materials, ferrihydrite is one of the more efficient, and widely used due to its specific physicochemical properties in removing both As (III) and As (V) [10,11]. However, the cost of preparation, limited availability of chemicals, and regeneration of ferrihydrite restrict its use in developing countries. Previous studies have explored the use of Balkuy laterite in treating arsenic-contaminated water [12,13]. Previous studies demonstrated that raw laterite collected in Balkuy district, showed a certain potential as an adsorbent of arsenic [14]. Moreover, prior research has demonstrated a significant correlation between the adsorption affinity of adsorbents rich in iron and arsenic [10,15]. The literature suggests that chemical pretreatment methods are effective in fixing ferrihydrite onto adsorbents [15,16,17]. Therefore, this study aimed to evaluate the efficiency of Balkuy laterite dopped with ferrihydrite for arsenic removal from water.

The objective of this study was to contribute to the safe drinking water supply in Burkina Faso using locally available materials to treat arsenic-contaminated water. Studying the arsenic removal under various conditions, the mechanisms and kinetics of arsenic removal in batch mode were investigated under various operating parameters.

2. MATERIALS AND METHODS

2.1 Chemicals

1000 ppm stock solution of arsenic (III) was prepared following to the method of Iman and *al.* [10] by dissolving sodium arsenite salt ($NaAsO_2$) with a 20% NaOH solution (Flucka). The solutions of arsenic (III) and arsenic (V) were prepared from the stock solutions of $NaAsO_2$ (Flucka) and $Na_2HAsO_4 .7H_2O$ (Merck), respectively, in ultra-pure distilled water for the different adsorption tests. These solutions were stored at 4°C in until used. NaOH (Flucka) and

HNO_3 (Sigma-Aldrich) reagents prepared in analytical grade (AR) were used to adjust the pH of the matrix solutions. The pH of arsenic solutions was adjusted between 7 and 8 using 1M NaOH and/or 1M HNO_3 with a pH- meter (HANNA, waterproof HI98318).

2.2 Preparations of Adsorbents

The raw laterite was collected in Balkuy district (12°17'23.35" N, 1°27'46.90" W), located close to Ouagadougou (Burkina Faso). The chemically treated laterite (TL) and the ferrihydrite-doped treated laterite (DL) were prepared according to the method described by of Dehou *and al.* [16] (Fig. 1). The grain size below 75 µm of the prepared adsorbents was used in the different tests. Mineral phases of raw laterite have been previously determined [14].

2.3 Physico-chemical Characterization of Adsorbents

Chemical analyses of the modified laterites were carried out by ICP-OES at the Bureau of Mines and Geology of Burkina (BUMIGEB). Experimentally, to 10 g of laterite, were added 5mL of nitric acid (68%, Flucka), 10 mL of hydrochloric acid (37%, Honeywell) and 5 mL of fluoridric acid. The mixture was placed on a hot plate at 175±5 °C until a cake formed in the 100 mL flask. The cake was then digested with 10 mL HCl and diluted with distilled water to the mark. The resulting solution was then diluted with distilled water. The structural morphology and surface chemical composition of the TL and DL adsorbents were analyzed using a scanning electron microscopy coupled with energy dispersive spectroscopy (SEM-EDX, Microspec-WDX 600/OXFORD). The Brunauer, Emmett, and Teller (BET) method was used to determine the specific surface area, Langmuir surface area, porosity, and pore size of TL and DL using a Micromeritics surface and pore size analyzer (TriStar II plus version 3.02). The surface functional groups of TL and DL were assessed by Fourier transform -infrared spectroscopy (FTIR, OUAFO driven by OPUS software) in the range of 4000 to 400 cm^{-1}. The powder of the modified laterites was determined by X-ray diffraction (XRD) using a Shimadzu XRD 6000 instrument. The scanning rate was set at 2 min^{-1} with a 2θ range between 0° and 90° [17,18]. To assess the amount of metal oxides present, Energy-Dispersive X-ray Fluorescence (EDXRF) was used to analyze the TL and DL adsorbents. Samples were irradiated by X-rays generated from the ^{109} Cd annular source. The Si (Li) detector (Canberra), cooled with liquid nitrogen, allowed for the detection of the characteristic X-ray radiation of the sample. The spectrum was collected using the Genie-2000 software (Canberra, Meriden, CT, USA). The WinAxil version 4.5.2 software (Canberra Eurisys Benelux, Belgium) was used to analyze the spectral data. Quantitative evaluation was performed using the characteristic Lα lines of the elements. The bulk densities (d) of the modified laterites were measured using a method described elsewhere [17]. The calculation of bulk density was performed using the following formula:

$$d = \frac{(m_1 - m_0)}{V} \quad (1)$$

The pH at the point of zero charge (pH_{PZC}) value was determined from the curve (initial pH – final pH) as a function of the initial pH intercepting the x-axis of pHi – pHf = 0 [19].

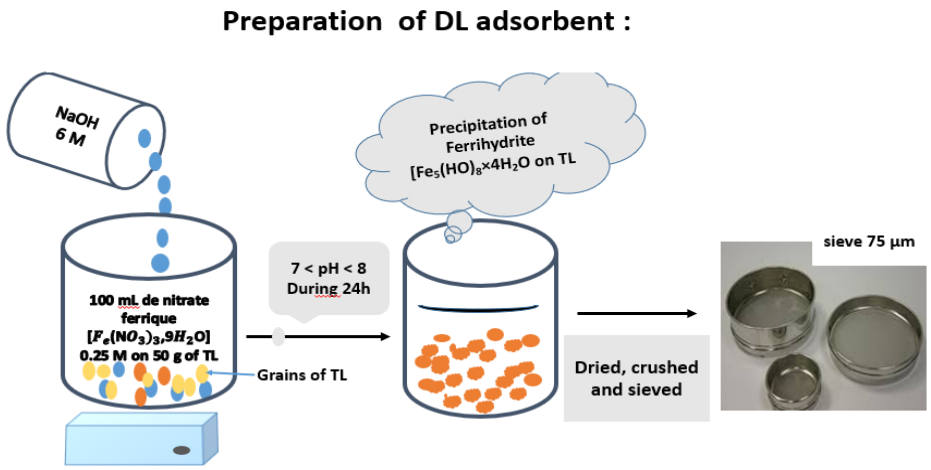

Fig. 1. Protocol for the preparation of DL laterite

2.4 Arsenic Removal Experiments

Batch experiments were conducted to assess the adsorption capacity and performance of the prepared adsorbents in removing As (III) and As (V). Experiments were carried out using a rotary mechanical shaker at 150 rpm at the laboratory's ambient temperature of 24 ± 0.15°C for 24 hours. An adsorbent dose of 4 g/L of TL or DL with a concentration of 5 mg/L of As (III) or As (V) was agitated with initial pH values adjusted between 2 to 12. The performance of modified laterites was evaluated by varying the mass dose over a range of 4 g/L to 14 g/L with a solution concentration of 5 mg/L of As (V) or As (III). The chemical equilibrium was studied by varying the initial concentration of As (V) or As (III) from 1 mg/L to 16 mg/L with an adsorbent dose of 4g/L of TL and DL. Adsorption kinetics experiments of As (III) or As (V) on TL and DL were conducted by performing tests from 01 to 24 hours with an adsorbent dose of 4g/L and As concentration of 5 mg/L. The residual arsenic was analyzed using a Microwave Plasma-Atomic Emission Spectrometer (MP-AES Agilent 4200) after filtration [20]. The adsorption efficiency of the prepared adsorbents on As (V) or As (III) was evaluated through the removal rate denoted As (%) and the adsorption capacity denoted Qe (mg/g).

The adsorption capacity (Qe) was determined by the following formula:

$$Q_e\left(\frac{mg}{g}\right) = \frac{(C_i - C_e) \times V}{m} \quad (2)$$

The removal percentage (%As) was calculated using the following relationship:

$$As\ (\%) = \frac{C_i - C_e}{C_i} \times 100 \quad (3)$$

3. RESULTS AND DISCUSSION

3.1 Physico-Chemical Characteristics of Prepared Adsorbents

The physical parameters of prepared adsorbents were presented in Table 1. From the results, no significant changed was observed in the total pore volume of the treated laterite vs the raw material. The increase in the value of density for DL was demonstrated through the contribution of iron during the doping of laterite (TL). Doping of TL by ferrihydrite has caused the closure of small pores by the binding of iron hydroxyls on the surface of these pores. In addition, the doping of TL by ferrihydrite has changed the surface charge, and the pH at the point of zero charge (pH_{PZC}) from acidic 5.41 to alkaline pH of 8.02 [17]. Regarding surface characteristics, the total specific surface area of DL has been reduced by half after the treatment. We observed a decrease in the BET and Langmuir surface values after TL doping, indicating a preference for iron hydroxyls to bind to the BET and Langmuir surfaces rather than the external surface. These results are in agreement with the studies of Glocheux *and al.* [18], who showed that porous materials such as treated laterite have an external surface and negligible porosity compared to the internal structure, hence the fixation of iron hydroxyls on the internal surface (BET and Langmuir surface). The variations in the values of physical parameters indicated that the doping of laterite with ferrihydrite contribute to physicochemical changes [18, 21].

The nitrogen (N_2) adsorption-desorption isotherms at 77K figure (Figs. 2a and 2b) revealed the distinct behaviour of the different TL and DL laterites. These adsorbents were correlated with the isotherm of type IV, characteristic of adsorbents with mesoporous pores of relatively uniform size (2 to 50 nm). This type of isotherm indicates rapid adsorption onto the TL and DL laterites at low pressures, followed by slower adsorption at higher pressures. According to the IUPAC (International Union of Pure and Applied Chemistry) classification, the presence of hysteresis in the isotherms of the three adsorbents indicates that the adsorption and desorption process is not reversible due to effects such as capillary condensation in narrow pores or adsorption on heterogeneous sites [17, 22]. These characteristics of the TL and DL laterites concluded that the adsorbents are highly permeable to water during the adsorption of As (III) and As (V).

Fig. 3 shows the surface functional groups of prepared adsorbents. Three zones of characteristic spectral bands are observed. The vibration zone around 3700 cm^{-1} corresponds to the O-H functional group. Three distinct peaks represent the bonds with Al^{3+}, Fe^{2+}, Fe^{3+}, and Ti^{4+} such as Fe-O, Al-O, Ti-O in the surface of the adsorbents [18, 21]. The second spectral band zone, the broad band around 1634 cm^{-1}, is attributable to isolated and bound water molecules on laterites. The broad peak around 2005 cm^{-1} on TL laterite is due to CO_2 adsorption [18]. The peaks around 1096, 910, 790, and 910 cm^{-1} confirmed the presence of characteristic Si-O bonds for both TL and DL laterites [23]. However, the bands around 530 and 460 cm^{-1} correspond to the vibration of the Fe-O bond of TL and DL [21, 23]. The intensity of the transmittance bands of the TL lateritewas attenuated compared to the DL after doping.

Table 1. Physical characteristics of TL and DL

Physical parameters	Quantitative values	
	T L	DL
Particle size (µm)	≤ 75 µm	
Density (d)	1.670	2.270
pH at zero point of charge pHpzc	5.410	8.020
Specific surface area BET (m^2/g)	24.548	7.995
Specific surface area of Langmuir (m^2/g)	30.208	10.688
Specific external surface area (m^2/g)	26.550	21.416
Total specific surface area (SS) (m^2/g)	81.306	40.099
Total pore volume (cm^3/g)	0.059	0.056

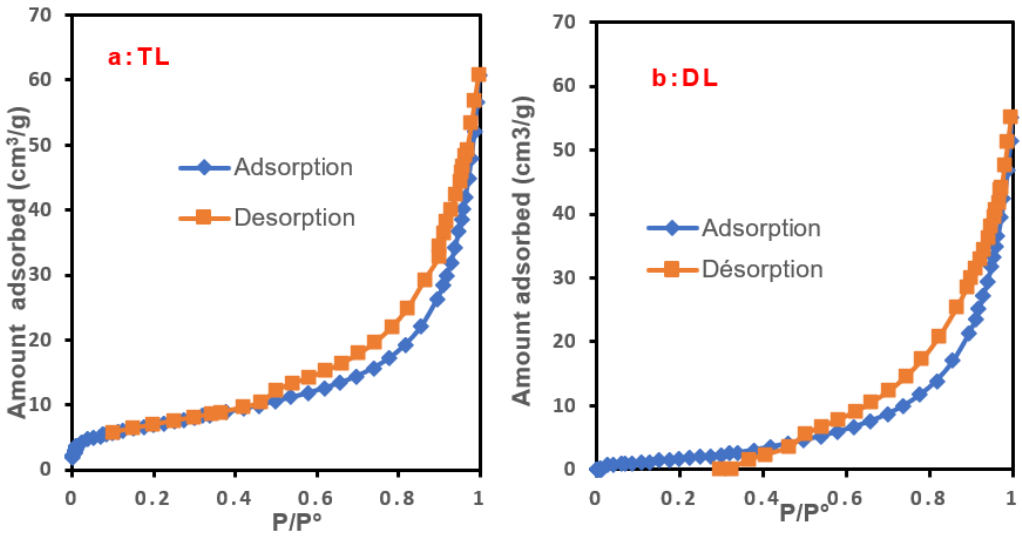

Fig. 2. Nitrogen (N_2) adsorption-desorption isotherms at 77 K for TL and DL

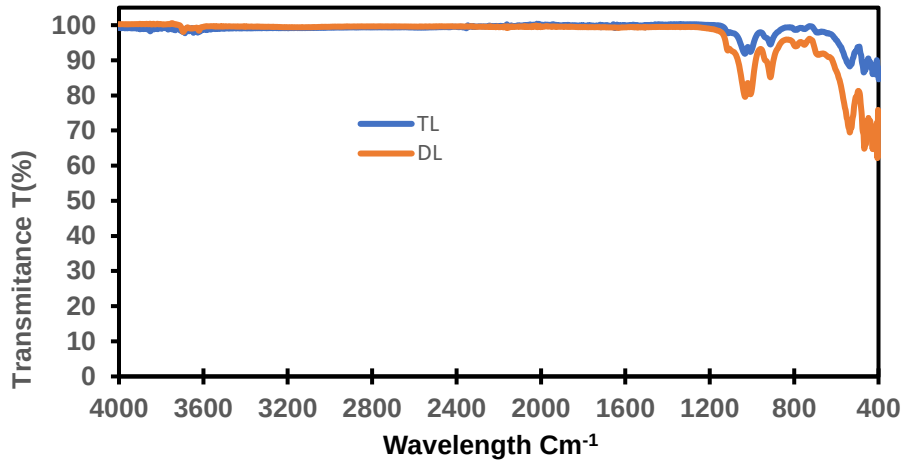

Fig. 3. FT-IR surface function analysis of TL and DL

XRD analysis of TL and DL showed that there were structural modifications after doping the treated laterite (Figs. 4a and 4b). Attributions of 2θ diffraction peaks to mineral phases were made through Powder Diffraction File Data Maps (PCPDF no. 290173 and 290712), available in the literature [18, 21]. Results revealed the presence of kaolinite, quartz, goethite, and hematite in TL laterite. In DL, in addition to previously cited phases, a significant amount of amorphous phase of 2-line ferrihydrite was observed on the diffractogram. The changes of the intensities of mineral phases in the diffractograms could indicate the performance of DL laterite for the adsorption of As (III) and As (V) compared with TL laterite [17].

SEM analysis of TL and DL adsorbents by at 10.0 µm scale is given in Fig. 5. Both adsorbents consist of irregularly agglomerated particles in the form of platelets. The platelets stacked on the TL and DL laterites would be the kaolinite [18]. The kaolinite platelets were less formed on DL comparatively to TL laterite. The incursions of whitish spherical shapes present on DL are probably attributable to goethite, hematite and ferrihydrite [21]. TL adsorbent exhibited larger pores compared to DL, which can be attributed to the presence of iron hydroxides from doping on distinct pore structures. This explained the increase in the specific surface area of TL compared to DL (Table 1). Results from FT-IR, XRD data, chemical analysis by ICP-OES, and EDXRF of the adsorbents were used to identify and quantify the elemental composition in the form of oxide [24]. Results were recorded in Table 2, which indicate that aluminium oxides, iron oxides, silica, and titanium are the main phases present in both adsorbents. The content of iron oxides was relatively higher in DL than TL, as a result of the fixation of iron after doping. A relative low value of silica, aluminium, and titanium in DL is due to the opening of pores during the fixation of iron oxides during the deposition of ferrihydrite [16,17]. $SiO_2/(Fe_2O_3 + Al_2O_3)$ ratio was 0.31 for TL adsorbent and 0.20 for DL laterite, which indicate that TL and DL can still be classified as lateritic adsorbents [14, 23].

Elemental surface chemical analysis of the TL and DL laterites was conducted using a 2.5 µm scale plate. Fig. 6 displays the EDX spectra of TL and DL as qualitative analysis. The surface elemental chemical composition of TL and DL as determined by EDX is presented in Table 2. The increase in silicon, carbon, iron, and aluminum content suggests that doping with ferrihydrite also improves the dispersion of these chemical elements in the adsorbent matrix. These EDX results provided further support for the XRD and EDXRF data. Moreover, the elemental composition of the prepared adsorbents was similar to other compositions reported in literature [14,17].

Table 2. Elemental chemical composition of TL and DL (%, m/m)

Oxides	SiO_2	Al_2O_3	Fe_2O_3	TiO_2	N_2O	MgO	CaO	ZnO, CuO, MnO_2
TL	19.07	25.62	36.31	1.82	4.45	4.85	2.05	≤ 1
DL	13.67	18.31	51.04	0.17	4.24	4.34	208	≤ 1

Elemental surface chemical analysis EDX

	O	C	Si	Al	Fe	Ti	Na	Ca
TL	51.43	17.52	6.24	7.73	5.62	17.52	0.11	0.39
DL	37.29	32.71	10.60	10.74	7.69	*	0.05	0.86

**Not determined*

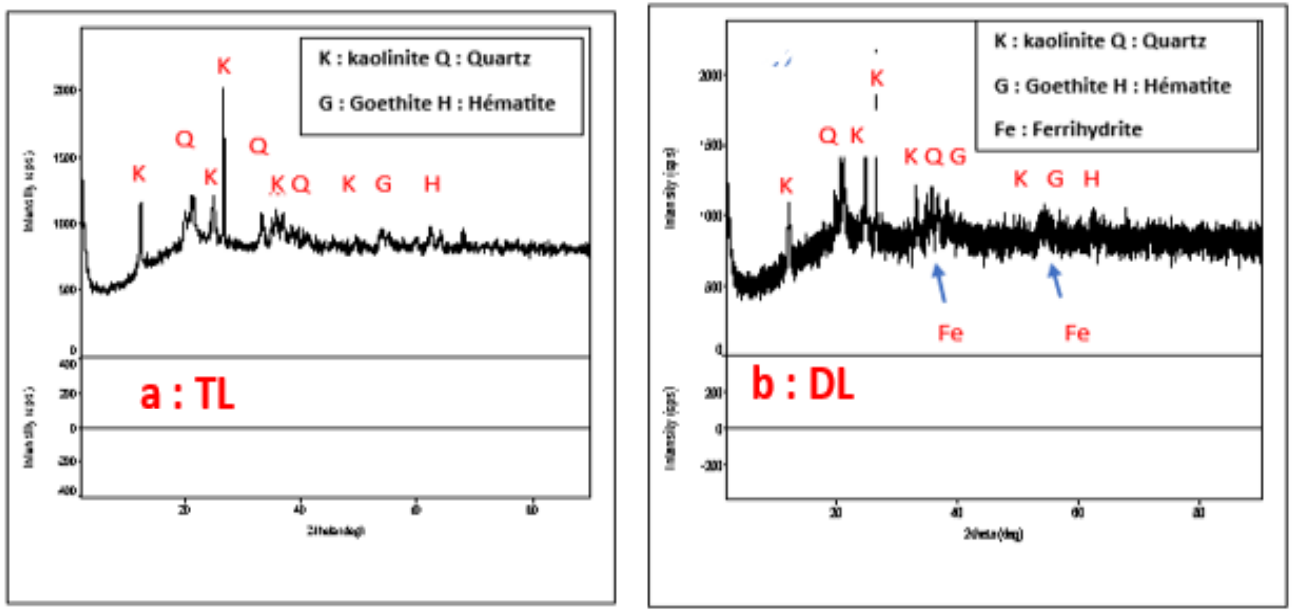

Fig. 4. Diffractogram of the mineral phases of TL and DL

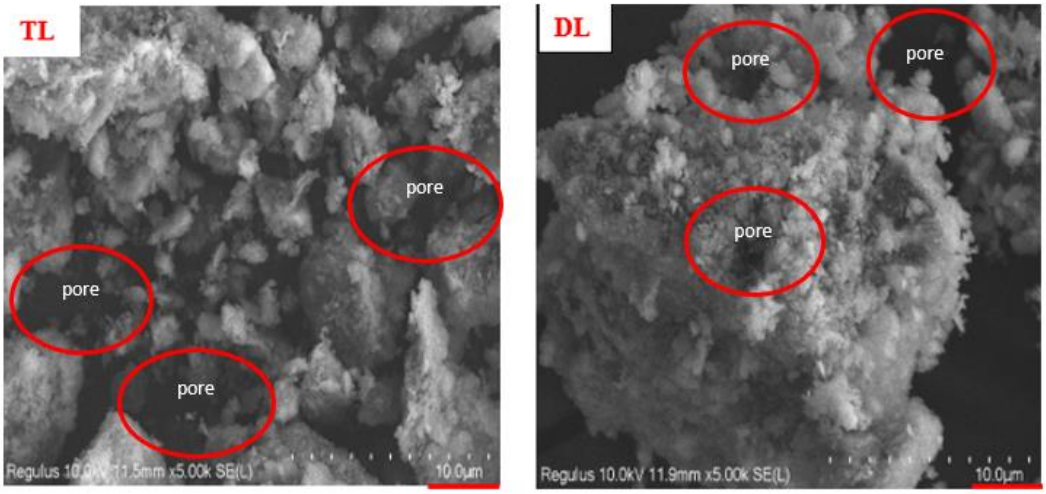

Fig. 5. SEM image of TL and DL adsorbents at 10.0 µm scale

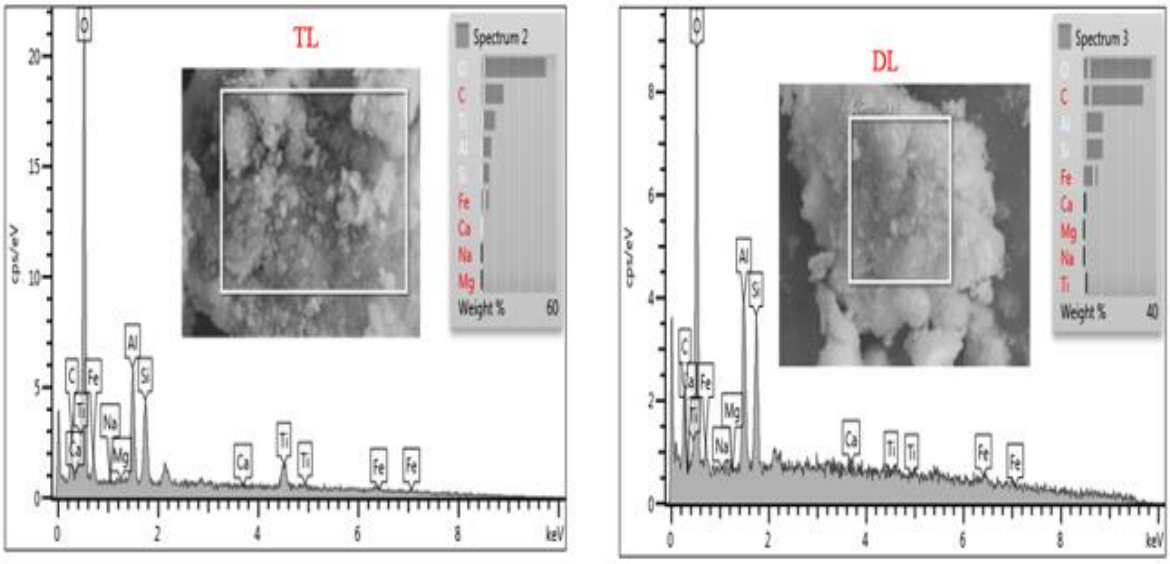

Fig. 6. EDX spectra of the TL and DL on a 2.5 µm scale SEM image

3.2 Effect of Operating Parameters on Arsenic Removal

3.2.1 Effect of initial pH of solution

The effect of pH on the removal of As (III) and As (V) is presented in Fig. 7. Optimal removal rate of As (V) on DL is achieved at a pH range between 4 and 8 with 99% of removal. Beyond a pH of ≥ PH_{PZC} (8.02) and at a pH below 4, the removal rate of As (V) gradually decreased. In contrast, using TL, the optimal pH was 5 with a removal rate of 90.30% of As (V). Above the pH_{PZC} (5.41) of TL, the removal rate of As (V) decreased from 88.98 to 38.86%. The removal of As (III) using adsorbents was not pH dependent in the range of pH = 2 to 10 because of its neutral form present in this pH range. The adsorption efficiency depends on the ionic forms of arsenic in solution (H_3AsO_4, $H_2AsO_4^-$, $HAsO_4^{2-}$, AsO_4^{3-}, H_3AsO_3, $H_2AsO_3^-$) and the adsorbents' point of zero charge (pH_{PZC}). For pH ≤ pH ($_{PZC}$) of adsorbents, the removal rate could be explained by the attraction process of of the anionic forms of As (V) to the positively charged surface of adsorbents. On the other hand, beyond the pH_{PZC} of adsorbents, the decrease in the removal rate indicates some repulsion of ionic forms of As (V) and hydroxyl ions on the negatively charged surface of adsorbents [13,17]. Low removal rates for As (III) compared to As(V) at the same pH could be due to its stability at pH < 9.2 and its

neutral form (H_3AsO_3) in solution, hence no electrostatic interaction on the surfaces [18]. The removal of As (III) on the surface of the adsorbents for pH comprised between 2 and 10 is mainly by ligand exchange, and electrostatic interaction is insignificant [18, 21]. The probable mechanism for the removal of As (III) and As (V) on TL and DL is that of Yang and *al.* [25], proposing ionisation of hydroxyls (-OH) on the adsorbent surface followed by complexation of the arsenic forms (bidentate and monodentate) on the adsorbent surfaces.

3.2.2 Effect of adsorbent dose

The effect of TL and DL dose on the removal of As (III) and As (V) was evaluated at adsorbent concentration from 4 to 40 g/L with an initial concentration of 5 mg/L at pH 7.05 for 24 hours contact time. Fig. 8 showed the increase in the removal rate of As (V) and As (III) on both adsorbents. The removal rate of As (V) increased from 59.84 to 95.72% using TL and from 78.32 to 98.20% using DL with the increase in adsorbent dose. In contrast, the removal rate of As (III) increased from 42.76 to 89.30% and from 33.40 to 95.70% respectively for TL and DL. High performance of TL was reached at 24 g/L for 87.28% of As (III) and 95.34% of As (V). Using DL, the optimal removal was for 90.88% of As (III) and 97.08% of As (V) with 16 g/L. From this result, the increase of arsenic removal indicates a more favourable adsorption of As (III) and As (V) using both two laterites. The increase in the rate removal of arsenic forms using DL was attributed to the addition of active sites resulting from the doping of TL [10,15].

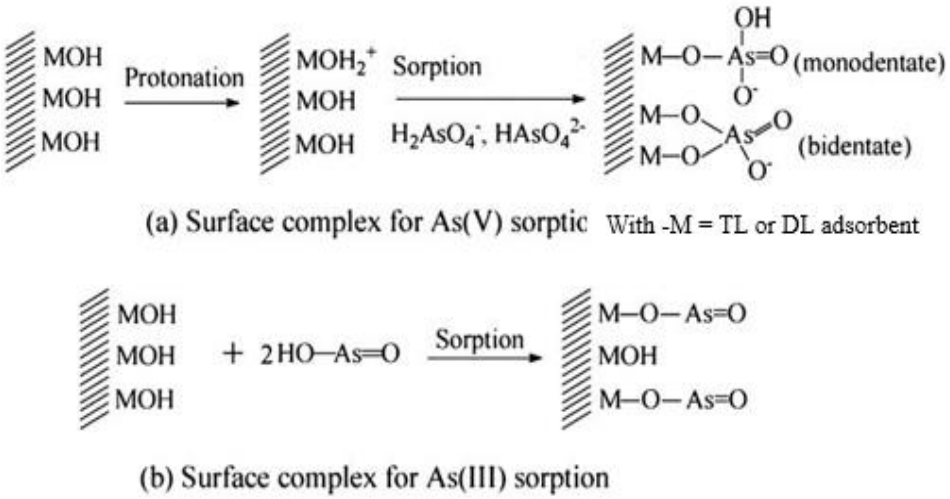

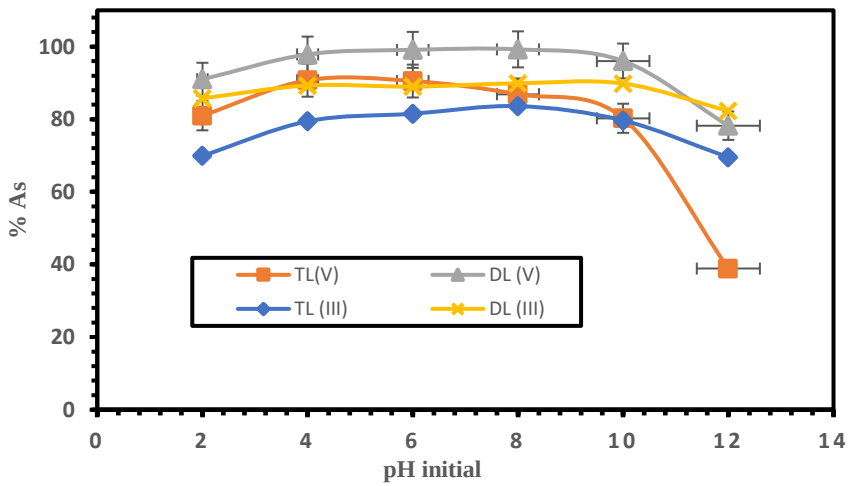

Fig. 7. Effect of initial pH on the removal of As (V) and As (III) with Co = 5mg/L, dose = 4g/L, and t = 24h

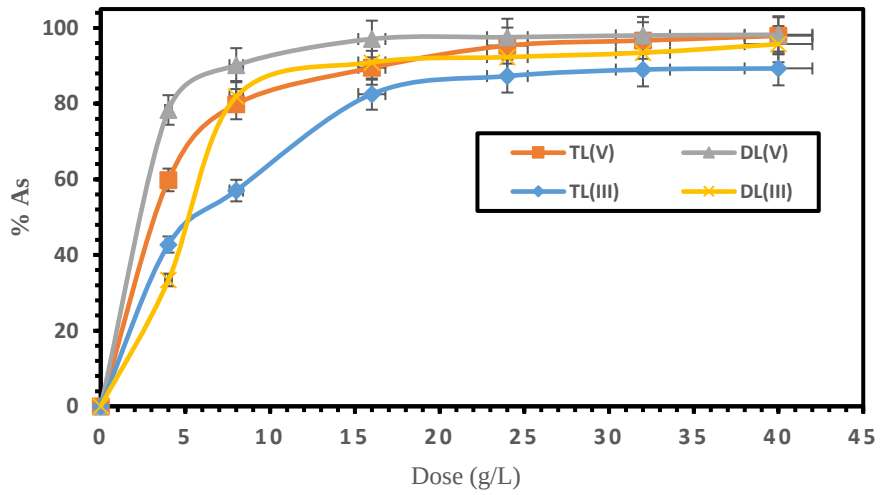

Fig. 8. Effect of adsorbent dose on the removal of As (V) and As (III) with Co = 5mg/L, pH = 7.05, and t = 24h

3.2.3 Effect of initial concentration

The adsorption behaviour of As (V) and As (III) onto TL and DL was carried out by varying the concentration between 2 and 16 mg/L at pH 7.11 with an adsorbent dose of 4 g/L during 24 hours contact time (Fig. 9). The removal rate of As (V) decreased from 100 to 85.62% and from 100 to 78.12% respectively using TL and DL. By removing As (III), the removal rate evolved from 100 to 65.62% and from 95 to 56.87% using TL and DL, respectively. The optimal initial concentration of As (V) and As (III) was respectively 6 mg/L and 4mg/L using TL. Using DL, the optimal removal was obtained at a initial concentration of 2 mg/L for As (V) and As (III). High performance of TL compared to DL could be explained by its high total specific surface area (approximately twice that of DL,) to fix more arsenic ions in solution [21, 24]. The progressive decrease in the removal rate of As (V) and As (III) is due to the limited number of active sites of the adsorbents during the increase in initial arsenic concentration [26].

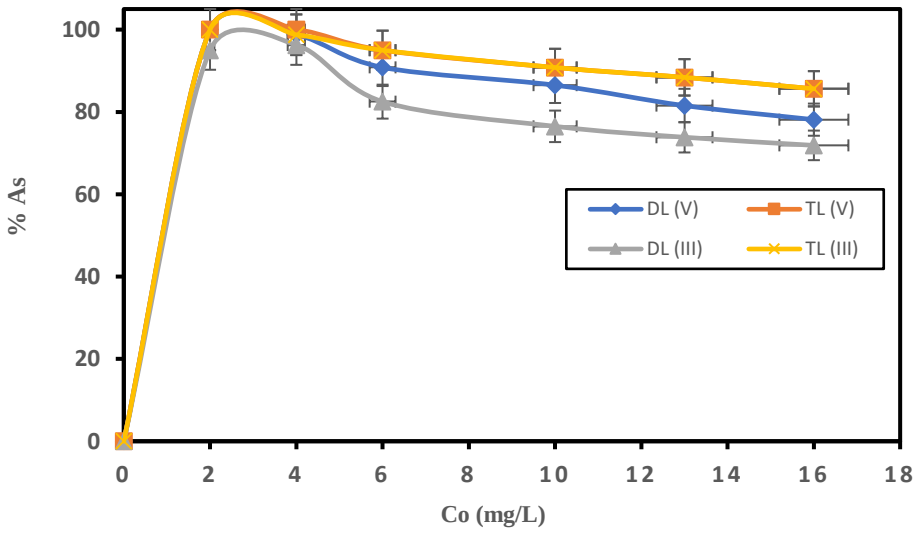

Fig. 9. Effect of initial concentration on the removal of As (V) and As (III), dose = 4 g/L, pH = 7.11, and t = 24 h

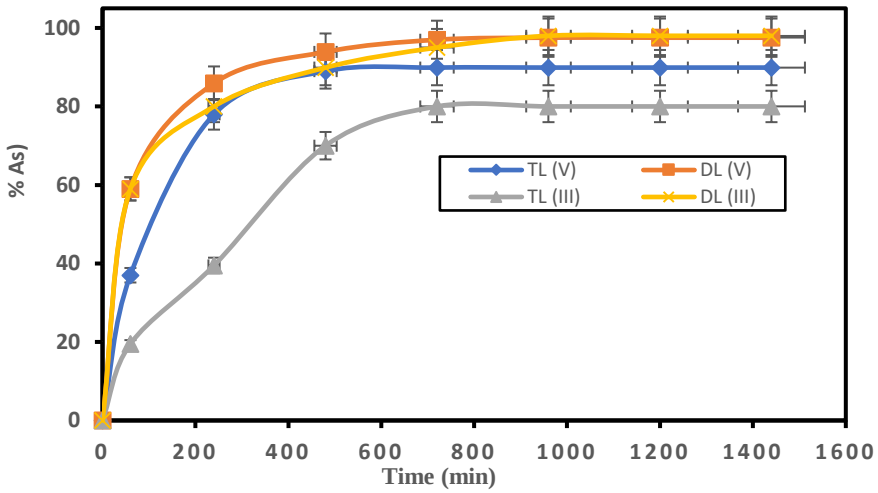

Fig. 10. Effect of initial time on the removal of As (V) and As (III), Co = 5 mg/L, dose = 4 g/L, and pH = 7.09

3.2.4 Effect of contact time

The influence of contact time was evaluated over 24 hours with an initial pH of 7.09 using TL and DL. The Fig. 10 shows the evolution of the removal rate of As (III) and As (V) according to two phases over time. During the first 4 hours, a rapid increase in the removal of As (III) and As (V) on the adsorbents was noted. For As (V), 79.47 and 95% of the removal rate were achieved using TL and DL, respectively. In contrast, the removal rate of As (III) was 39.45 and 79.47% using TL and DL, respectively. This rapid removal was due to the availability of free active sites of the adsorbents at the beginning of the adsorption process [14,17]. After 4 hours, the removal of As (III) and As (V) on the TL and DL laterites reached chemical equilibrium. The adsorption rate then remained constant. At equilibrium, the performance of DL was 97.67% and 100% for As (III) and As (V) respectively. Using TL laterite, the performance was 81.24% and 95.05% for As (III) and As (V) respectively at equilibrium time. This equilibrium performance of DL could be explained by the physicochemical surface properties allowing for the gradual removal of the initial concentration of As (III) and As (V) over time. The saturation of active sites of TL could be explained by the chemical equilibrium reached, indicating that it is not possible to increase the arsenic removal with the evolution of time [18, 26].

3.2.5 Kinetic modeling

To study the kinetic mechanism of treated laterite (TL) and doped laterite (DL), experimental data obtained with influence of contact time, were linearized with the models of pseudo-first order and pseudo-second order, respectively described by Lagergren *and al.* [27] and by Ho and Mckay [28] for the adsorption of As (V) and As (III). The integration of the equations gives the following formulas respectively:

$$\text{Ln } (Qe - Qt) = - k_1\, t + \text{ln } Qe \qquad (4)$$

$$\frac{t}{Q_t} = \frac{1}{Q_e} t + \frac{1}{K_2\, Qe^2} \qquad (5)$$

The representations of these equations are given by the Fig. 11:

Values of the kinetic constants are listed in Table 3 where we noticed the experimental and theoretical capacity of each laterite. In addition, the values of correlation coefficient R^2 is given for expected comparison.

The comparison between the experimental adsorption capacity (Qe_{exp}) and calculated (Qe_{theo}) of the first-order and pseudo-second-order is given in Table 3. Using the pseudo-second-order model, values of correlation coefficient (R^2) were higher compared to the pseudo-first-order model. In addition, the calculated values of adsorption capacities Qe_{theo} are close to the experimental values (Qe_{exp}) with the pseudo-second-order model. All these results indicated that the adsorption of As (III) and As (V) using two TL and DL adsorbents was described by the pseudo-second-order kinetic. The mechanism of As (III) and As (V) removal could then be describe by chemisorption process [17, 29].

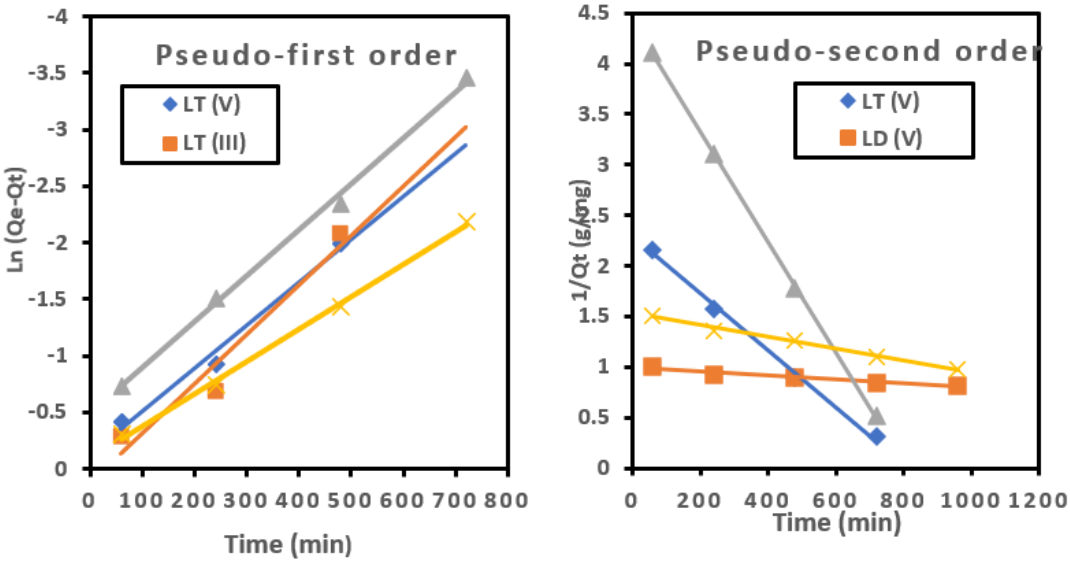

Fig. 11. Representation of the kinetic models of arsenic removal onto TL and DL

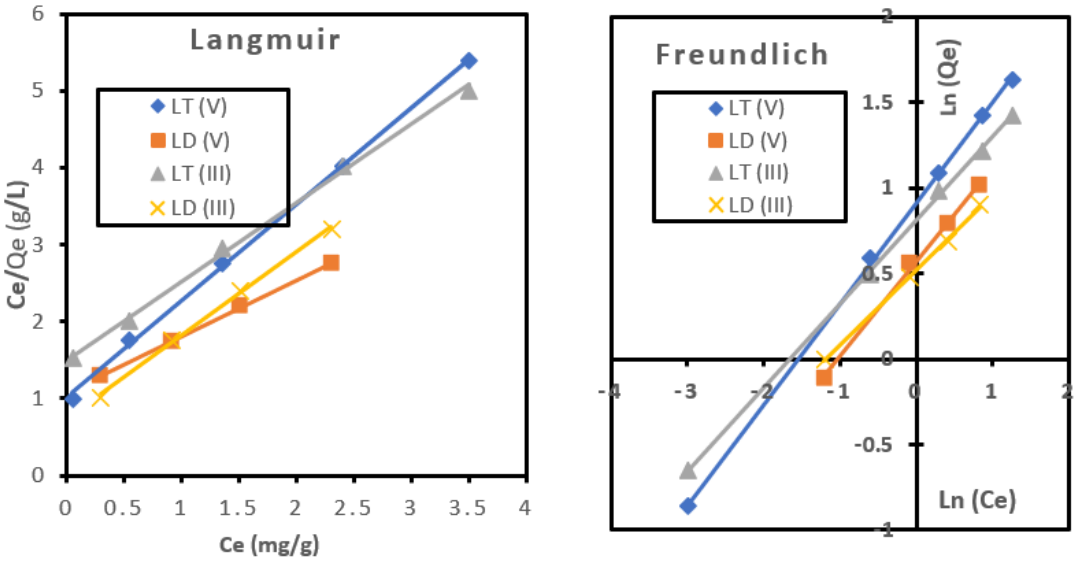

Fig. 12. Representation of the isotherm models of As (V) and As (III) removal on TL and DL

Table 3. Kinetic constants for pseudo-first and pseudo-second order

Adsorbent	Pseudo-first order				Pseudo-second order			
	Qe_{exp}	$Qe_{théo}$	K_1	R^2	Qe_{exp}	$Qe_{théo}$	K_2	R^2
	mg/g	mg/g	min^{-1}		mg/g	mg/g	min^{-1}	
TL (V)	0.72	0.27	0.008	0.91	0.72	0.70	0.14	0.98
DL (V)	0.89	0.21	0.010	0.93	0.89	0.90	0.38	0.99
TL (III)	0.68	0 .17	0.006	0.87	0.68	0.67	0.12	0.98
DL (III)	0.76	0.19	0.007	0.96	0.76	0.77	021	0.98

Table 4. Langmuir and Freundlich constants for arsenic removal) using TL and DL

Adsorbent	Langmuir			Freundlich		
	Q_m (mg/g)	K_L (L/mg)	R^2	K_f (mg/g)	n	R^2
TL (V)	7.36	0.73	0.98	5.06	1.78	0.97
DL (V)	9.79	0.28	0.99	6.31	3.46	0.98
TL (III)	5.17	1.01	0.99	2.98	1.09	0.98
DL (III)	7.89	0.38	0.99	4.01	2.72	0.99

3.2.6 Adsorption isotherms modelling

The adsorption behavior of As (V) and As (III) onto TL and DL as a function of the initial concentration was linearized to the Langmuir and Freundlich isotherms [22, 30]. The monolayer adsorption capacity on homogeneous active sites of TL and DL was studied using the Langmuir model; and multilayer adsorption on heterogeneous sites was evaluated using the Freundlich model for As (III) and As (V) [30]. The linearized form of the Langmuir isotherm model is given by the relation (6):

$$\frac{C_e}{Q_e} = \frac{1}{Q_m}(C_e) + \frac{1}{K_L Q_m} \quad (6)$$

The equation of the Freundlich model is given by the following relation (7):

$$LnQ_e = lnK_f + \frac{1}{n} lnC_e \quad (7)$$

Fig. 12 shows the plots $Ce/Qe = f(Ce)$ and $LnQe = f(LnCe)$ for Langmuir and Freundlich, respectively. The slopes and intercepts of the curves were used to calculate the various constants of isotherm models. Data of isotherm models are recorded in Table 4.

The R^2 constants of Langmuir and Freundlich isotherms are between 0.97 and 0.99 using TL and DL, indicating a good correlation and possible exploitation of experimental data for the removal of As (III) and As (V). The values of maximum capacities (Q_m) and affinity constants (n) of Langmuir and Freundlich respectively recorded in Table 4 show an affinity and favorable reaction between the different mineral phases of the two adsorbents and the forms of arsenic. Consequently, the removal of As(III) and As(V) could be occurred by multilayer adsorption. The equilibrium parameter R_L and the Gibbs free energy (ΔG) were evaluated from the following relationships based on the Langmuir isotherm [30].

$$\Delta G = -RTLn\, K_L \quad (8)$$

$$R_L = \frac{1}{1+K_L C_O} \quad (9)$$

The calculated R_L values were between 0 and 1 with negative Gibbs free energies between 1.23 and 3.14 kJ/mole indicating the removal of As(III) and As(V) was occurred by adsorption following a reversible process onto TL and DL laterites [31-34].

4. CONCLUSION

In this work, we reported the improvement of the properties of a laterite by analytical preparation techniques of TL and DL. Characterization by physico-chemical methods of the adsorbents allowed to observe structural modifications with surface functions. The presence of kaolinite, quartz, goethite, and hematite was observed on the treated laterite, and in addition to these mineral phases, ferrihydrite was identified on the doped treated laterite. Batch adsorption tests showed that the efficiency of TL and DL adsorbents in the removal of As (V) and As (III) depended on operating conditions (initial pH, adsorbent dose, initial concentration, and initial time). The mechanisms of removal of As (V) and As (III) on TL and DL were described by multilayer adsorption occurred onto heterogenous surfaces of DL and TL with not located sites. Kinetic study of adsorption of As (V) or As (III) onto adsorbents followed the pseudo-second-order model.

DISCLAIMER (ARTIFICIAL INTELLIGENCE)

Author(s) hereby declare that NO generative AI technologies such as Large Language Models (ChatGPT, COPILOT, etc) and text-to-image generators have been used during writing or editing of manuscripts.

ACKNOWLEDGEMENTS

The Authors would like to thank the SENEXEL laboratory and the BUMIGEB for their support in MP-AES and ICP-OES analyses of adsorbents. The World Academy of Sciences for advancement of sciences in developing countries and United Nations organization for Education

and Culture (UNESCO) are gratefully acknowledged for the research grant No. 22-087 RG/CHE/AF/AC_I FR 3240325133, enabling to carry out this study.

COMPETING INTERESTS

Authors have declared that no competing interests exist.

REFERENCES

1. Sayan B, Avishek T, Shubhalakshmi S, Tuyelee D, Abhijit D, Kaushik G, et al. Arsenic contaminated water remediation: A state-of-the-art review in synchrony with sustainable development goals. Groundwater for Sustainable Development. 2023;23:2352-801X. DOI:https://doi.org/10.1016/j.gsd.2023.101000.
2. Smedley PL, Knudsen J, Maiga D. Arsenic in groundwater from mineralized Proterozoic basement rocks of Burkina Faso. Appl Geochem. 2007;22:1074-92. DOI:https://doi.org/10.1016/j.apgeochem.2007.01.00.
3. Ollé RK, Corneille B, Inoussa Z, Boubié G. Assessing the source of thallium contamination in ground and surface waters in the locality of Yamtenga (Burkina-Faso): Correlation with some heavy metal ions. Int Res J Pure Appl Chem. 2019;19:1-14. DOI:https://doi.org/10.9734/IRJPAC/2019/v19i430122.
4. Ackmez M, Sanjay KS, Vinod KG, Chin HT. Arsenic: An overview of applications, health, and environmental concerns and removal processes. Crit Rev Environ Sci Technol. 2011;41:435-519. DOI:http://dx.doi.org/10.1080/10643380902945771.
5. Bretzler A, Lalanne F, Nikiema J, Podgorski J, Pfenninger N, Berg M, et al. Groundwater arsenic contamination in Burkina Faso, West Africa: Predicting and verifying regions at risk. Sci Total Environ. 2017;584-585:958-70. DOI:https://doi.org/10.1016/j.scitotenv.2017.01.147.
6. Tiendrebéogo R, Sanou Y, Paré S, Senou A. Preparation and characterization of ferrihydrite: Application in arsenic removal from aqueous solutions. Asian J Chem Sci. 2024;14:27-39. DOI:https://doi.org/10.9734/ajocs/2024/v14i3307.
7. Somé IT, Sakira AK, Ouédraogo M, Ouédraogo TZ, Traoré A, Sondo B, et al. Arsenic levels in tube-wells water, food, residents urine and the prevalence of skin lesions in Yatenga province, Burkina Faso. Interdiscip Toxicol. 2012;5:38-41. DOI: https://doi.org/10.2478/v10102-012-0007-4.
8. Arunima N, Priya C, Brij B, Kapil G, Seema S, Mika S. Removal of emergent pollutants: A review on recent updates and future perspectives on polysaccharide-based composites vis-à-vis traditional adsorbents. Int J Biol Macromol. 2024;258:0141-8130. DOI:https://doi.org/10.1016/j.ijbiomac.2023.129092.
9. Sanou Y, Pare S. Arsenic pollution through drinking groundwater in Burkina Faso: research of a cheap removal technology. In: Nolasco M, Carissimi E, Urquieta-Gonzalez E, editors. Water perspectives in emerging countries: linking water security to sustainable development goals. Göttingen: Cuvillier Verlag. 2018;137-48.
10. Inam MA, Khan R, Lee KH, Akram M, Ahmed Z, Lee KG, et al. Adsorption capacities of iron hydroxide for arsenate and arsenite removal from water by chemical coagulation: Kinetics, thermodynamics and equilibrium studies. Molecules. 2021;26:7046. DOI:https://doi.org/10.3390/molecules26227046.
11. Qi P, Pichler T. Closer look at As (III) and As (V) adsorption onto ferrihydrite under competitive conditions: Langmuir. J Am Chem Soc. 2014;30:11110-6. DOI: https://doi.org/10.1021/la502740w.
12. Sanou Y, Kabore R, Pare S. Adsorption of arsenic and phosphate from groundwater onto a calcined laterite as fixed bed in column experiments. Fr-Ukr J Chem. 2020;8(2):227-42. DOI:https://doi.org/10.17721/fujcV8I2P227-243.
13. Sanou Y, Tiendrebeogo R, Pare S. Développement d'un pilote de traitement des eaux de forage contaminées par l'arsenic pour une application en zones rurales au Burkina Faso. J West Afr Chem Soc. 2020;49:22-30.
14. Sanou Y, Kolawole CB, Tiendrebeogo R, Kabore R, Tchakala I, Pare S. Physico-chemical and spectroscopic properties of

two laterite soils for applications in arsenic water treatment. Int J Multidiscip Res Dev. 2020;7:12-7.

15. Mahler J, Persson I. Rapid adsorption of arsenic from aqueous solution by ferrihydrite-coated sand and granular ferric hydroxide. Appl Geochem. 2013;37:179-89. DOI:https://doi.org/10.1016/j.apgeochem.2013.07.025.
16. Dehou SC. Etude des propriétés d'adsorption des oxyhydroxydes de fer déposé sur un support naturel (la brique): application à l'élimination du fer dans les eaux de forages en République Centrafricaine [dissertation]. Lille: Université Lille 1; 2011.
17. Sanou Y. Etude de la performance des charbons actifs, du granulé d'hydroxyde ferrique et de la latérite pour l'élimination de la demande chimique en oxygène, du calcium et de l'arsenic des eaux. Doctoral thesis, Ouagadougou: Université Ouaga I Pr Joseph KI-ZERBO; 2017.
18. Glocheux Y, Méndez M, Albadarin B, Allen J, Walker MG. Removal of arsenic from groundwater by adsorption onto an acidified laterite by-product. Chem Eng J. 2013;228:565-74. DOI:https://doi.org/10.1016/j.cej.2013.05.043.
19. Reymond JP, Kolenda F. Estimation of the point of zero charge of simple and mixed oxides by mass titration. Powder Technol. 1999;103:30-6. DOI: https://doi.org/10.1016/S0032-5910(99)00011-X.
20. Azhar AG, Zuhair AAK, Kasim HK. Selective extraction and determination of arsenic (III) and arsenic (V) in some food samples by cloud-point extraction coupled with hydride generation atomic absorption spectrometry. Int Res J Pure Appl Chem. 2014;4:362-77.
21. Chatterjee S, De S. Application of novel, low-cost, laterite-based adsorbent for removal of lead from water: Equilibrium, kinetic and thermodynamic studies. J Environ Sci Health A Tox Hazard Subst Environ Eng. 2016;51:193-203. DOI:https://doi.org/10.1080/10934529.2015.1094321.
22. Rahman M, Lamb D, Rahman M, Bahar M, Sanderson P. Adsorption-desorption behavior of arsenate using single and binary iron-modified biochars: Thermodynamics and redox transformation. J Am Chem Soc Omega. 2022;7:101-17. DOI:https://doi.org/10.1021/acsomega.1c04129.
23. Boccuzzi F, Chiorino A, Manzoli M, Andreeva D, Tabakova T. FTIR study of the low-temperature water–gas shift reaction on Au/Fe2O3 and Au/TiO2 catalysts. J Catal. 1999;188:176-85. DOI:https://doi.org/10.1006/jcat.2001.3290.
24. Njoya D, Njoya A, Kamlo NA, Tchuindjang YD, Nkoumbou C. Caractérisation chimique et minéralogique de quelques indices de bauxite de Foumban (Ouest-Cameroun). Int J Biol Chem Sci. 2017;11:444. DOI: https://doi.org/10.4314/ijbcs.v11i1.35.
25. Yang Y, Ling Y, Kok YK, Chenghong W, Chen JP. Rare-earth metal-based adsorbents for effective removal of arsenic from water: A critical review. Crit Rev Environ Sci Technol. 2018;48:1127-64. DOI: 10.1080/10643389.2018.1514930.
26. Tasrina RC, Amin MN, Quraishi SB, Mustafa AI. Arsenic (III) removal from real-life groundwater by adsorption on neem bark (*Azadirachta indica*). Int Res J Pure Appl Chem. 2014;46:594-604.
27. Abinashi S, Jeongwon P, Hyoeun K, Pyung KP. Arsenic removal from aqueous solutions by adsorption onto hydrous iron oxide-impregnated alginate beads. J Ind Eng Chem. 2016;35:277-8. DOI:https://doi.org/10.1016/j.jiec.2016.01.005.
28. Tasrina RC, Acher T, Amin MN, Quraishi SB, Mustafa AI. Removal of arsenic (III) from groundwater by adsorption onto duckweed (*Lemna minor*). Int Res J Pure Appl Chem. 2015;6:120-7. DOI:https://doi.org/10.9734/IRJPAC/2015/12798.
29. Alhaji MIN, Tajun MBMK. Optimization and kinetic study for the removal of chromium (VI) ions by acid treated sawdust chitosan composite beads. Int Res J Pure Appl Chem. 2014;5:160-76. DOI:https://doi.org/10.9734/IRJPAC/2015/13834.
30. Langmuir I. The adsorption of gases on plane surfaces of glass, mica and platinum. J Am Chem Soc. 1918;40:1361-403. DOI:http://dx.doi.org/10.1021/ja02242a004
31. Melisa A, Indira S, Amra O, Edisa P, Husejin K, Abdel D, et al. The potential of bentonite as a low-cost adsorbent for the

removal of heavy metal ions from multicomponent aqueous systems of the galvanic industry. Int Res J Pure Appl Chem. 2024;25:28-39. DOI:https://doi.org/10.9734/IRJPAC/2024/v25i2848.

32. Hema KR. Comparative studies of isotherm and kinetics on the adsorption of Cr (VI) and Ni (II) from aqueous solutions by powder of mosambi fruit peelings. Int Res J Pure Appl Chem. 2013;4:26-45. DOI:https://doi.org/10.9734/IRJPAC/2014/5765.

33. Mohan D, Pittman Jr CU. Arsenic removal from water/wastewater using adsorbents—a critical review. J Hazard Mater. 2007;142(1-2):1-53.

34. Al-Ghouti MA, Da'ana DA. Guidelines for the use and interpretation of adsorption isotherm models: A review. J Hazard Mater. 2020;393:122383.

Peer-review history:
The peer review history for this paper can be accessed here:
https://www.sdiarticle5.com/review-history/119483